Nuclear Engineering and Technology 53 (2021) 1893–1908

Contents lists available at ScienceDirect

Nuclear Engineering and Technology

journal homepage: www.elsevier.com/locate/net

Original Article

A new burn-up module for application in fuel performance calculations targeting the helium production rate in $(U,Pu)O_2$ for fast reactors

A. Cechet, S. Altieri, T. Barani, L. Cognini, S. Lorenzi, A. Magni, D. Pizzocri, L. Luzzi*

Politecnico di Milano, Department of Energy, Nuclear Engineering Division, Via La Masa 34, 20156, Milano, Italy

ARTICLE INFO

Article history:
Received 21 August 2020
Received in revised form
22 November 2020
Accepted 1 December 2020
Available online 5 December 2020

Keywords:
Burn-up module
Oxide nuclear fuels
Fuel performance code
SCIANTIX
Helium production

ABSTRACT

In light of the importance of helium production in influencing the behaviour of fast reactor fuels, in this work we present a burn-up module with the objective to calculate the production of helium in both in-pile and out-of-pile conditions tracking the evolution of 23 alpha-decaying actinides. This burn-up module relies on average microscopic cross-section look-up tables generated via SERPENT high-fidelity calculations and involves the solution of the system of Bateman equations for the selected set of actinide nuclides. The results of the burn-up module are verified in terms of evolution of actinide and helium concentrations by comparing them with the high-fidelity ones from SERPENT, considering two representative test cases of $(U,Pu)O_2$ fuel in fast reactor conditions. In addition, a code-to-code comparison is made with the independent state-of-the-art module TUBRNP (implemented in the TRANSURANUS fuel performance code) for the same test cases. The herein presented burn-up module is available in the SCIANTIX code, designed for coupling with fuel performance codes.

1. Introduction

Fuel and cladding materials undergo isotopic and microstructural evolution during reactor operation, affecting fuel pin performance and safety [1]. As burn-up increases, the change of the fuel isotopic composition directly causes production of inert gases, whose evolution in the grains and at the grain boundaries leads to gaseous swelling and gas release in the pin free volume. Such phenomena affect the integrity of the fuel pin, modifying the dimensions of the fuel pellets, the fuel-cladding gap conductance, and pin internal pressure [2–4]. On the other hand, the variation of fuel composition strongly influences some crucial properties for the fuel performance analysis, such as thermal conductivity, melting (solidus) temperature, heat capacity, elastic modulus, and thermal expansion. Thus, a reliable prediction of actinide evolution and inert gas production in nuclear fuels is required as input for models which aim to represent the changes in the fuel thermal and mechanical properties. This is even more relevant in the framework of the development of future Generation IV reactor concepts and related fuel materials, where the target fuel burn-up is higher compared with the present technologies [5,6].

In the frame of a fuel performance simulation, the resolution of neutron transport is hardly affordable[1] because it would require access to microscopic cross-sections libraries, with cross-sections as function of the incident neutron energy, angle, fuel pin composition, excessively increasing the overall computational cost of a fuel pin simulation. Since in fuel performance calculations the focus is only on nuclides relevant to determine the radial power profile in the fuel pellet, and on helium production as well, the approach conventionally adopted is to evaluate once and for all the set of needed average cross-sections for different fuel/reactor combinations. To do this, databases of averaged microscopic cross-sections have been generated coupling neutron transport codes (e.g., MCNP [7]) with depletion codes (e.g., ORIGEN [8]) [3,4]. For example, the RADAR module of Palmer et al. [9], embedded in the ENIGMA fuel performance code and called in every node of the

* Corresponding author.
E-mail address: lelio.luzzi@polimi.it (L. Luzzi).

[1] Monte Carlo burn-up calculation codes, as well as many deterministic ones, adopt coupling schemes in which at every burn-up step sequential steady-state neutronics solutions and depletion calculations with constant microscopic reaction rates are combined into a burn-up calculation, thus implying significant overall computational times. This stepwise approach is adopted for example in the SCALE [37] and PHISICS [38] codes, where TRITON and INSTANT are the neutronics modules and ORIGEN [8] and MRTAU are the depletion modules, respectively.

https://doi.org/10.1016/j.net.2020.12.001

mesh, consists of: (1) a differential equation for the local ^{235}U concentration, (2) a differential equation for the local ^{239}Pu concentration, and (3) the solution of a simple diffusion theory for the thermal neutron flux. The main disadvantage is that it considers only the formation of ^{239}Pu, while the formation of ^{240}Pu and higher plutonium isotopes is neglected. With the purpose of extending the RADAR module and its predictions of experimental plutonium build-up, the TUBRNP module, embedded in the TRANSURANUS fuel performance code [10], has been developed. In TUBRNP, the effective cross-sections for neutron-induced fissions and captures in UO_2 fuel depend on the reactor type and on the enrichment of ^{235}U, while the related cross-sections for LWR-MOX (uranium-plutonium mixed oxide) fuel depend on the initial Pu concentration [11]. The resonance absorption of neutrons in ^{238}U and ^{240}Pu[2] is considered implicitly via a radial form factor [10,12,13]. Recently, the module was extended to Th-based LWR fuels by Tijero Cavia et al. [14]. Further worth-mentioning burn-up modules developed for fuel performance calculations are RAPID [15], PLUTON (part of ASFAD, FEMAXI-V and MACROS fuel performance codes [16]), RTOP [17] and the burn-up module of the COSMOS code [18]. In addition, the DIONISIO code [19] has been developed and recently extended to model the fuel behaviour at high burn-up [20,21]. Fundamental developments to include the production of helium in burn-up modules applicable in fuel performance codes were performed by Federici et al. [22] (PRODHEL code) and Botazzoli et al. [23] (TUBRNP code extension). Both include the description of ^{238}Pu, ^{242}Cm and ^{244}Cm as main α-emitters, yet not tracking explicitly ^{242}Am and ^{242m}Am, whose effect on ^{242}Cm production is crucial to achieve a good description of helium, especially when a certain plutonium and minor actinide concentration is present in the fresh fuel.

In this work, we present a burn-up module suitable for application in fuel performance codes, developed within the SCIANTIX code, an open source intermediate-scale code developed to describe fission gas behaviour at the fuel grain level [24]. SCIANTIX aims at effectively bridging the lower-length scale of atomistic simulations and the engineering scale of fuel performance codes, feeding the latter with theoretical and experimental knowledge about fission gas behaviour mechanisms, always complying with the computational requirements of fuel performance codes. In addition, it aims at being useable as a stand-alone code for the simulation of separate-effect experiments at the fuel-grain scale involving inert gas behaviour, both supporting the design of the experiment itself and the interpretation of the results. As already declared, the development of this burn-up module has a twofold purpose, namely, to predict both the helium production and the actinide evolutions in oxide fuels in fast reactor irradiation conditions. These objectives are particularly important for $(U,Pu)O_2$ fuels for fast reactors, since the initial enrichment in plutonium nuclides leads to a relevant content of minor actinides (which are mostly α-emitters and hence helium-producers). The focus of the present work, grafted within the INSPYRE Project [25], is therefore on Pu-bearing oxide fuels, whereas the burn-up module itself and the methodology used to develop it can be applied to any kind of fuel/reactor combinations. Compared to state-of-the-art modules currently available in fuel performance codes, we choose to include the evolution of a high number of nuclides, like ^{242}Am and ^{242m}Am, aiming at a more detailed and accurate description of helium production. The proposed methodology consists in coding multi-dimensional look-up tables for each relevant cross-section. The entries for these look-up tables are obtained from SERPENT calculations [26], a 3D continuous-energy Monte Carlo reactor physics and burn-up calculation code, through the computation of the reaction rate integrals (RRI). Every cross-section is calculated for a selected burn-up range and various initial Pu/HM (heavy metal) contents and is collected in a proper look-up table.[3] This methodology has been applied to $(U,Pu)O_2$ fuel in two different reactor conditions, namely, sodium fast reactor (MOX/SFR) and lead-bismuth eutectic fast reactor (MOX/LBE-FR).[4] Since the database of cross-sections is embedded in SCIANTIX, the herein presented burn-up module can be either used as a stand-alone code or coupled with fuel performance codes. In this work, we use this module as stand-alone, but the coupling between SCIANTIX and TRANSURANUS fuel performance code is currently under development [27,28].

This paper is organized as follows. In Section 2, we formulate the general structure of the burn-up module. In Section 3, we provide an in-depth view of the methodology applied to develop the module itself, while in Section 4 we assess its predictions in terms of helium and actinide concentrations (benchmarking it against both SERPENT and TUBRNP).

2. Outline of the burn-up module structure

The uranium isotopes considered in this burn-up module are ^{234}U, ^{235}U, ^{236}U, ^{237}U and ^{238}U. ^{233}U belongs to the neptunium series, the so-called $4n+1$ series, and undergoes α-decay into ^{229}Th, which in turn decays into lighter nuclei: it is therefore quite irrelevant in the production of transuranic elements, except for the (n,γ) reaction which creates ^{234}U. In addition, ^{233}U is produced by β-decay of ^{233}Pa, which derives from the α-decay of ^{237}Np whose half-life ($t_{1/2}$) is about 2.14 million years. In view of its limited production rate paired to its long half-life of 159.2 ky for α-decay, ^{233}U has been neglected and the lighter uranium isotope herein considered is ^{234}U. ^{239}U (which is produced only by (n,γ) reaction with ^{238}U) transmutes into ^{239}Np, and consequently into ^{239}Pu. Because of the short β-decay time of ^{239}U compared to the other uranium isotopes ($t_{1/2} = 26.6$ min), it is neglected in the chain with the assumption that ^{239}U becomes immediately ^{239}Np.

Considered neptunium isotopes are ^{237}Np, ^{238}Np and ^{239}Np. ^{240}Np is produced only from (n,γ) reaction on ^{239}Np. The latter has a low half-life for what concerns its β-decay into ^{239}Pu. For these reasons, this isotope has been neglected.

As for plutonium, in the module we consider the isotopes from ^{238}Pu to ^{243}Pu. Although produced in relative negligible quantity, ^{243}Pu undergoes β-decay ($t_{1/2} = 4.95$ h) producing the α-emitter ^{243}Am, hence it is considered in the model.

Moreover, this burn-up module tracks ^{241}Am, ^{242}Am, ^{242m}Am, ^{243}Am and ^{244}Am as americium isotopes. It is well known that ^{242m}Am has a relatively long half-life ($t_{1/2} = 141$ years), therefore its inclusion in the burn-up module is crucial because of its role in the production path of the α-emitter ^{242}Cm [29].

Finally, the considered curium isotopes are ^{242}Cm, ^{243}Cm, ^{244}Cm and ^{245}Cm, which are all strong α-emitters. ^{246}Cm is not included in line with the considerations made by Botazzoli et al. [23,30], who proved that the evolution of the transuranic elements until ^{245}Cm is sufficient for a satisfactory description of helium evolution due to

[2] In addition, TUBRNP considers the burn-up dependence of the ^{240}Pu neutron capture cross-section.

[3] It is worth mentioning that also the ORIGEN code, developed at Oak Ridge National Laboratories, uses fuel/reactor-dependent cross-section look-up tables for depletion calculations [8].

[4] It should be underlined that a direct coupling of SERPENT and TRANSURANUS codes has been developed for the simulation of Gd-doped UO_2 in the frame of the ESSANUF Project [39], and that a similar coupling in the open source SALOME platform for nuclear reactor simulations is under development in the frame of the McSAFE Project [40].

α-decays in the framework of fuel performance codes.

To summarize, the present version of the module considers α and β decays for each nuclide, the internal transition of ^{242m}Am and the electronic capture of ^{242}Am. Some decay processes have been neglected because of branching ratios lower than 1% (e.g., all the spontaneous fissions and the α-decay of ^{241}Pu, with a branching ratio of 0.00245%) [31]. Instead, reactions that involve neutrons are fissions, radiative captures, and neutron multiplications, such as (n,2n) and (n,3n). These latter reactions are significant only for high energy neutrons and have very low average cross-sections, but must be considered in the evolution of ^{234}U, ^{236}U and ^{237}U [32,33].[5] It is worth noticing that the number of nuclides and neutron reactions (especially neutron multiplication reactions) considered in this work is limited, since the inclusion of all the possible reaction channels would have implied a rise in the computational time for the depletion calculation, not compliant with requirements of industrial fuel performance codes.

As detailed before, among the actinides described by the present module, several are α-emitters and hence are the main contributors to helium production in nuclear fuel under irradiation, together with (n,α) reactions on ^{16}O and ternary fissions, as detailed by Federici [22] and Botazzoli [23,30]. The resulting equation for helium evolution is:

$$\begin{aligned}\frac{d\left[^4\mathrm{He}\right]}{dt} &= \lambda_{\alpha,^{234}\mathrm{U}}\left[^{234}\mathrm{U}\right] + \lambda_{\alpha,^{235}\mathrm{U}}\left[^{235}\mathrm{U}\right] + \lambda_{\alpha,^{236}\mathrm{U}}\left[^{236}\mathrm{U}\right] + \lambda_{\alpha,^{238}\mathrm{U}}\left[^{238}\mathrm{U}\right] \\ &+ \lambda_{\alpha,^{237}\mathrm{Np}}\left[^{237}\mathrm{Np}\right] \\ &+ \lambda_{\alpha,^{238}\mathrm{Pu}}\left[^{238}\mathrm{Pu}\right] + \lambda_{\alpha,^{239}\mathrm{Pu}}\left[^{239}\mathrm{Pu}\right] + \lambda_{\alpha,^{240}\mathrm{Pu}}\left[^{240}\mathrm{Pu}\right] + \lambda_{\alpha,^{242}\mathrm{Pu}}\left[^{242}\mathrm{Pu}\right] \\ &+ \lambda_{\alpha,^{241}\mathrm{Am}}\left[^{241}\mathrm{Am}\right] + \lambda_{\alpha,^{243}\mathrm{Am}}\left[^{243}\mathrm{Am}\right] \\ &+ \lambda_{\alpha,^{242}\mathrm{Cm}}\left[^{242}\mathrm{Cm}\right] + \lambda_{\alpha,^{243}\mathrm{Cm}}\left[^{243}\mathrm{Cm}\right] + \lambda_{\alpha,^{244}\mathrm{Cm}}\left[^{244}\mathrm{Cm}\right] + \lambda_{\alpha,^{245}\mathrm{Cm}}\left[^{245}\mathrm{Cm}\right] \\ &+ \sigma_{n,\alpha\,^{16}\mathrm{O}}\varphi\left[^{16}\mathrm{O}\right] + y_{\mathrm{TF}}\dot{F} \end{aligned} \quad (1)$$

where $\left[^{\mathrm{i}}\mathrm{X}\right]$ (at m^{-3}) is the concentration of the nuclide $^{\mathrm{i}}$X, $\lambda_{\alpha,\,^{\mathrm{i}}\mathrm{X}}$ (s^{-1}) is the α decay constant of the nuclide $^{\mathrm{i}}$X, $\sigma_{n,\alpha\,^{16}\mathrm{O}}$ (m^2) is the cross-section for the (n,α) reaction with ^{16}O, φ (m^{-2} s^{-1}) is the local neutron flux, y_{TF} is the ternary fission yield, set equal to 0.22% [31], and $\dot{F}$ (fiss m^{-3} s^{-1}) is the local fission rate density.

All the father-to-daughter relations between the nuclides considered in the proposed burn-up module are represented in Fig. 1.

3. Methodology

One of the main advantages brought about by the proposed burn-up module is the standardized development methodology, which can be applied to different oxide nuclear fuels and different kind of reactors. The methodology is depicted in Fig. 2 and can be summarized as follows:

1. Run a set of SERPENT calculations with different initial fuel compositions, representative of the analysed fuel/reactor combination.
2. For each initial Pu/HM enrichment e_0, collect the values of microscopic cross-sections at different burn-up values (e.g., $bu = 0, 5, 10, 15, \ldots$GWd/t$_{\mathrm{HM}}$), evaluated by the calculation of the reaction rate integrals (RRI) in the Monte Carlo simulation.
3. Each microscopic cross-section is now available at discrete sampling points as a function of the initial enrichment e_0 and local burn-up bu, e.g., the cross-section for reaction r of nuclide $^{\mathrm{i}}$X will be a discrete function $^{\mathrm{Xi}}\overline{\sigma}_r(e_0, bu)$.
4. These discrete functions are expressed as two-entry tables and coded as look-up tables in a dedicated SCIANTIX routine.

These steps are to be performed once and for all, i.e., are necessary at the beginning for the inclusion of the cross-section look-up tables in SCIANTIX (OFFLINE, Fig. 2). The extraction of the cross-section values following the detailed methodology and the subsequent implementation of the look-up tables in SCIANTIX bring about a more accurate description of the depletion process with respect to using a fixed value for the cross-sections during fuel burn-up, which is the approach adopted, for example, in TUBRNP [10,12,23]. The set of Bateman equations (one for each nuclide considered) is then solved by SCIANTIX at each time-step (ONLINE, Fig. 2). Since the SCIANTIX burn-up and Pu/HM enrichment values are in general different from those used in SERPENT for the generation of the look-up tables, an interpolation within the values collected in the look-up tables is required.

First, we employed SERPENT offline calculations to equip SCIANTIX with the cross-section look-up tables, useful to calculate the nuclide concentration evolutions during fuel burn-up (under defined irradiation conditions). The tables depend on the fuel/reactor combination, since the average cross-sections depend on the neutron energy spectrum, which in turn is determined by the whole reactor characteristics. SERPENT uses the collision estimate of neutron flux to calculate user-defined reaction rates integrated over space and energy (RRI):

$$R = \frac{1}{V}\int_V\int_E f(\mathbf{r}, E')\varphi(\mathbf{r}, E')d^3r dE' \quad (2)$$

where V (m^3) is the volume of the target material, E (eV) is the user-defined energy grid, $f(r, E')$ is the response function to be evaluated and $\varphi(r, E')$ (m^{-2} s^{-1} eV^{-1}) is the space- and energy-dependent neutron flux. In SERPENT, the absolute value of the RRI depends on source normalization. In this work, for each test-case, we used a power density of 40 kW kg^{-1} (which corresponds

[5] The ^{238}U(n,3n)^{236}U reaction is present in the ^{236}U evolution equation, while it is absent in the ^{238}U equation because of its very low relative cross-section value (~10^{-5} b).

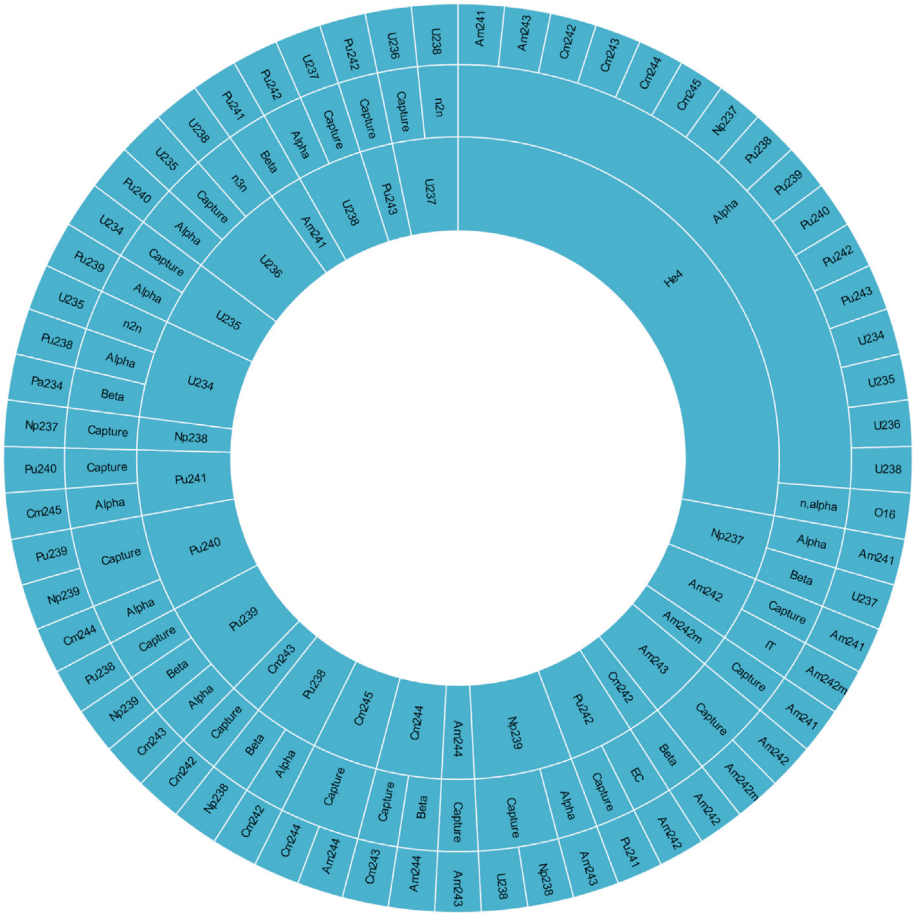

Fig. 1. Father-to-daughter relations between the 23 nuclides and helium considered in SCIANTIX. In the inner and outer circles, the daughter nuclide and the parent nuclide are reported, respectively. The middle circle indicates the relation (i.e., nuclear reaction) between the parent and the daughter nuclides. Since ^{239}U, ^{240}Np and ^{245}Am are short-lived nuclides, they have been excluded from the scheme.

to a fission rate density of 1.32 10^{19} fiss m^{-3} s^{-1}, assuming 208 MeV fiss^{-1}) to normalize the source. To compute the microscopic averaged cross-sections, the response function number expressed in ENDF format[6] has been set and the result normalized to the neutron flux. In this way, we calculated the cross-sections as:

$$ {}^{iX}\overline{\sigma}_r(e_0, bu) = \frac{\int_V \int_E {}^{iX}\sigma_r^i(e_0, bu, E')\varphi(\mathbf{r}, E')d^3rdE'}{\int_V \int_E \varphi(\mathbf{r}, E')d^3rdE'} \quad (3) $$

where ^{i}X, e_0 and bu are the considered target nuclide, the initial plutonium enrichment of the fuel and the burn-up, respectively, $^{Xi}\sigma_r(e_0, bu, E')$ (m^2) is the set of microscopic cross-sections, which is a function of burn-up bu, initial fuel enrichment e_0 and incident neutron energy E', while $\varphi(r, E')$ (m^{-2} s^{-1} eV^{-1}) is the neutron flux per energy as function of the neutron energy E' and space.

The SERPENT simulation is performed for a single fuel pin, modelled as having a cylindrical geometry (fuel pellet) in a prismatic space (coolant), with a reflective boundary condition on the coolant external surface. In the test cases performed, the initial fuel (MOX) composition is chosen based on standard isotopic compositions which would likely be similar to those adopted for the Gen-IV ASTRID (sodium-cooled fast reactor) and MYRRHA (LBE-cooled fast reactor) concepts [34]. The cladding material is 15-15 Ni–Cr, Ti stabilized, stainless steel (SS), adopted in the French SFR.

The depletion calculation is performed in 41 equally distanced burn-up steps of 5 GWd/t$_{HM}$ until 200 GWd/t$_{HM}$ for each case. The initial fuel composition accounts for a value of Pu/HM enrichment which goes from 20% to 40% with steps of 2%. The initial neutron population is set to 10′000 neutrons for both cases, with 100 active neutron generations and 30 inactive generations. The solution of the burn-up matrix in SERPENT is achieved through the Chebyshev Rational Approximation Method (CRAM) [35], while we use linear extrapolation as predictor method and linear interpolation as corrector method for what concerns the time integration method in burn-up calculations. All the cross-sections generated by the offline depletion calculation with SERPENT are collected in SCIANTIX in look-up tables (i.e., as a function of the peculiar nuclide, reaction, initial plutonium enrichment and local burn-up). For the sake of completeness, the main features used to build the SERPENT simulations for the two fuel/reactor cases herein analysed are reported in Table 1.

As for the implementation in SCIANTIX, the depletion of the nuclides presented in Section 2 is divided in two steps: first, the calculation of the actual cross section for each isotope and neutron flux value; second, the numerical solution of the set of Bateman

[6] The ENDF format uses special numbers to define reaction types [41]. In this work we used the values corresponding to total fissions (18), first chance fissions (19), neutron captures (102) and neutron multiplication reactions (16,17).

equations to find the fuel composition at the end of the SCIANTIX time step. In a SCIANTIX simulation, an interpolation to derive every cross-section value at the current fuel burn-up is required, since the cross-section values are collected in the look-up tables as discretized in SERPENT burn-up and enrichment steps, as previously mentioned. The cross-section corresponding to a SCIANTIX burn-up/enrichment couple, called e_{target} and bu_{target} below, is between four discrete values of SERPENT burn-up/enrichment couples. The target couple and the square edges define four rectangles whose areas are proportional to the weight of the cross-sections in the opposite corner. In this way, we build the target cross-sections as a weighted sum of the four nearest cross-sections in the look-up table:

$$ {}^{\mathrm{X}}\overline{\sigma}_r(e_{\text{target}}, bu_{\text{target}}) = {}^{\mathrm{X}}\overline{\sigma}_r(e_1, bu_1)\, A_{22} + {}^{\mathrm{X}}\overline{\sigma}_r(e_1, bu_2)\, A_{21} + {}^{\mathrm{X}}\overline{\sigma}_r(e_2, bu_1)\, A_{12} + {}^{\mathrm{X}}\overline{\sigma}_r(e_2, bu_2)\, A_{11} \tag{4} $$

where A_{ij} are the areas of the rectangles, calculated as:

$$ A_{mn} = \left|(e_{target} - e_m)\left(bu_{target} - bu_n\right)\right| \tag{5} $$

This expression is evaluated for each time step and for every cross-section.

The local, mono-energetic neutron flux is obtained from the fission rate density (input of the SCIANTIX code) as follows. First, the approximated one-group macroscopic fission cross-section $\overline{\Sigma}_f$ (m^{-1}) is obtained as:

$$ \overline{\Sigma}_f = \sum_{i \in \text{fissile}} {}^{\mathrm{Xi}}\overline{\sigma}_f \left[{}^{\mathrm{i}}\mathrm{X}\right](t_i) \tag{6} $$

where ${}^{\mathrm{Xi}}\overline{\sigma}_f$ (m^2) is the one-group microscopic fission cross-section of the ${}^{\mathrm{i}}$X nuclide and $\left[{}^{\mathrm{i}}\mathrm{X}\right](t_i)$ (at m^{-3}) is the concentration of the ${}^{\mathrm{i}}$X nuclide at the beginning of the SCIANTIX time step. Once computed the one-group macroscopic fission cross-section $\overline{\Sigma}_f$, the local flux at each time step is calculated as follows [20]:

$$ \overline{\varphi} = \frac{\dot{F}}{\overline{\Sigma}_f} \tag{7} $$

where $\dot{F}$ (fiss $\mathrm{m}^{-3}\ \mathrm{s}^{-1}$) is the local fission rate density set by input.

The last operation required in the SCIANTIX code is the solution of the Bateman equations, i.e., the depletion calculation itself. Since this last operation is decoupled from the generation of the microscopic cross-sections, it is essentially the solution of a system of linear ordinary differential equations (ODEs), namely:

$$ \frac{d}{dt}\left[{}^{\mathrm{i}}\mathrm{X}\right] = \sum_{r,j} {}^{\mathrm{Xj}}\overline{\sigma}_r(e_0, bu)\overline{\varphi}\left[{}^{\mathrm{j}}\mathrm{X}\right] - \sum_{r} {}^{\mathrm{Xi}}\overline{\sigma}_r(e_0, bu)\overline{\varphi}\left[{}^{\mathrm{i}}\mathrm{X}\right] + \sum_{d,k} \lambda_{d,k}\left[{}^{\mathrm{k}}\mathrm{X}\right] - \sum_{d} \lambda_{d,i}\left[{}^{\mathrm{i}}\mathrm{X}\right] \tag{8} $$

where the first summation accounts for the reactions r on nuclides ${}^{\mathrm{j}}$X resulting in ${}^{\mathrm{i}}$X, the second summation accounts for the reactions r on nuclide ${}^{\mathrm{i}}$X, the third summation accounts for the decays d of nuclides ${}^{\mathrm{k}}$X resulting in ${}^{\mathrm{i}}$X, and the fourth summation accounts for the decays d of nuclide ${}^{\mathrm{i}}$X.

It is worth noticing that the SCIANTIX burn-up module does not require the application of predictor-corrector methods, since the cross-sections have been pre-calculated for each SERPENT burn-up step. In fact, the choice of decoupling the local neutron flux from the nuclide concentrations (i.e., applying an operator-splitting procedure, estimating the neutron flux assuming unchanged isotopic compositions prior to the depletion calculation) allows for a saving of the computational cost with respect to the iterative solution of the system of ODEs represented by Eq. (8). This assumption is deemed acceptable, in light of the primary application of the burn-up module to the estimation of the helium source for the SCIANTIX inert gas behaviour models, thus needing to preserve a computational effort in-line with requirements of engineering-scale fuel performance codes. Following such considerations, we choose the backward Euler numerical method to integrate the ODE system in SCIANTIX, consistently with the SCIANTIX numerical scheme. The choice of the backward Euler method is dictated by (a) the limited number of considered nuclides, (b) the enforcement of adequately small time steps compatible with the different time scales governing the nuclide evolution, and (c) the consistency with the SCIANTIX numerical framework, which is built upon a consistent choice of the backward Euler method for the integration of ODEs.

Finally, it must be underlined that the production of helium (Eq. (1)) is handled in two steps: the part that involves only the alpha decays and the (n,α) reactions is solved together with the actinide burn-up equations, while the contribution given by the ternary fission yield multiplied by the fission rate density is separately added to the helium concentration obtained from the first step.

4. Assessment of SCIANTIX predictions

The assessment of the methodology presented in Section 3 has been carried out following two steps: first, a comparison between SCIANTIX with its high-fidelity source SERPENT; second, a code-to-code comparison between SCIANTIX and TUBRNP[7], the burn-up module implemented in the TRANSURANUS fuel performance code.

We carried out with the SCIANTIX code the simulations of the

[7] Corresponding to the TRANSURANUS version v1m1j18.

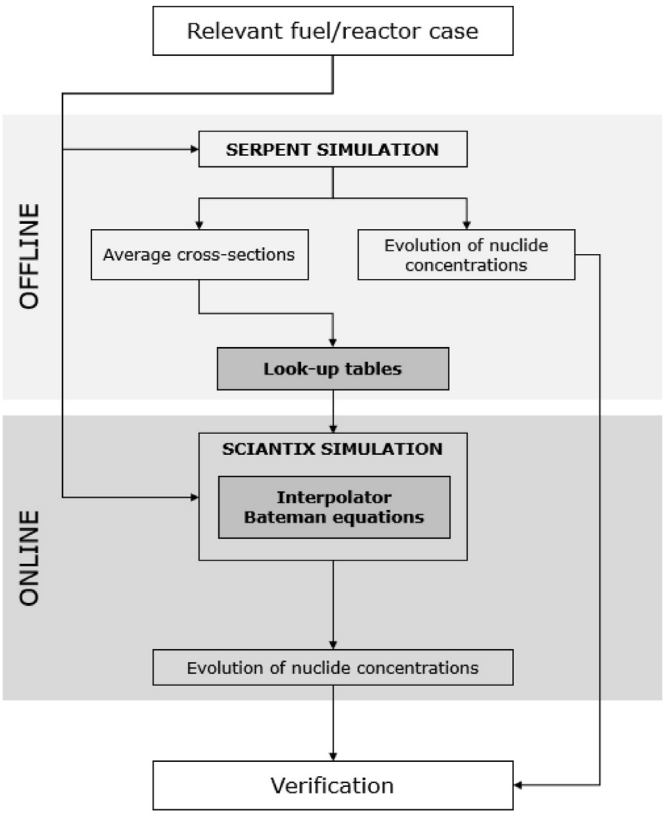

Fig. 2. Methodology applied for the generation of the cross-section look-up tables by SERPENT (OFFLINE), the solution of the depletion calculation in SCIANTIX (ONLINE) and the consequent comparison of results (verification).

Table 2
Main SCIANTIX parameters set for the simulation of the two test-cases.

Parameter	MOX/SFR	MOX/LBE-FR
Number of history points	8	8
Number of time step per history point	1′000	1′000
Irradiation time (h)	106′000	106′000
Burn-up at discharge (GWd/tHM)	200	200
Fission rate density (fiss m^{-3} s^{-1})	$1.32 \cdot 10^{19}$	$1.32 \cdot 10^{19}$
Grain radius (m)	$10 \cdot 10^{-6}$	$10 \cdot 10^{-6}$
Fuel density (g cm^{-3})	10.97	10.97
O/HM	1.975	1.97
Fuel composition: atoms per HM atom (in %)		
^{235}U	0.6	0.6
^{238}U	79.4	79.4
^{238}Pu	0.5	0.5
^{239}Pu	11.3	11.3
^{240}Pu	5.4	5.4
^{241}Pu	1.2	1.2
^{242}Pu	1.6	1.6

Table 3
Comparison between TUBRNP and SCIANTIX execution time.

Execution time (s)	TUBRNP	SCIANTIX
MOX/SFR	0.80	0.65
MOX/LBE-FR	0.61	0.66

same SERPENT cases, and we compared the results to assess the proposed burn-up module.[8] The irradiation lasts approximately 106′000 h, corresponding to 12 years, for both MOX/SFR and MOX/LBE-FR cases. In Table 2, the main SCIANTIX initial conditions employed for the simulations are listed.

Table 1
Value of the main SERPENT input parameters set for the derivation of the cross-section look-up tables. Each couple of Pu/HM and burn-up values corresponds to a specific cross-section value.

Parameter	MOX/SFR	MOX/LBE-FR
External pellet radius (mm)	2.71	2.71
Radial gap (mm)	0.115	0.115
U/HM (%)	80–60[a]	80–60[a]
Pu/HM (%)	20–40[b]	20–40[b]
Enrichment step width (at/HM %)	2	2
O/HM	1.97	1.97
Fuel density (g cm^{-3})	10.97	10.97
Column length (mm)	650	650
Cladding material	15-15 Ti SS	15-15 Ti SS
Cladding thickness	0.45	0.45
Cladding density (g cm^{-3})	7.95	7.95
Coolant	Sodium	Lead–Bismuth Eutectic (Pb 45 wt%, Bi 55 wt%)
Coolant prism side (mm)	6.7	6.7
Coolant prism height (mm)	670	670
Coolant density (g cm^{-3})	0.61[c]	10.28[c]
Total burn-up (GWd/t_{HM})	200	200
Burn-up step width (GWd/t_{HM})	5	5
Burn-up steps	41	41
Power density (kW kg^{-1})	40	40

[a] Assumed natural uranium isotopic composition.
[b] ^{238}Pu/Pu 2.332%, ^{239}Pu/Pu 56.873%, ^{240}Pu/Pu 26.997%, ^{241}Pu/Pu 6.105%, ^{242}Pu/Pu 7.693% (in wt.%).
[c] From Sobolev [36].

[8] The results shown refer to a Pu/HM concentration of 20%, for both MOX/SFR and MOX/LBE-FR cases.

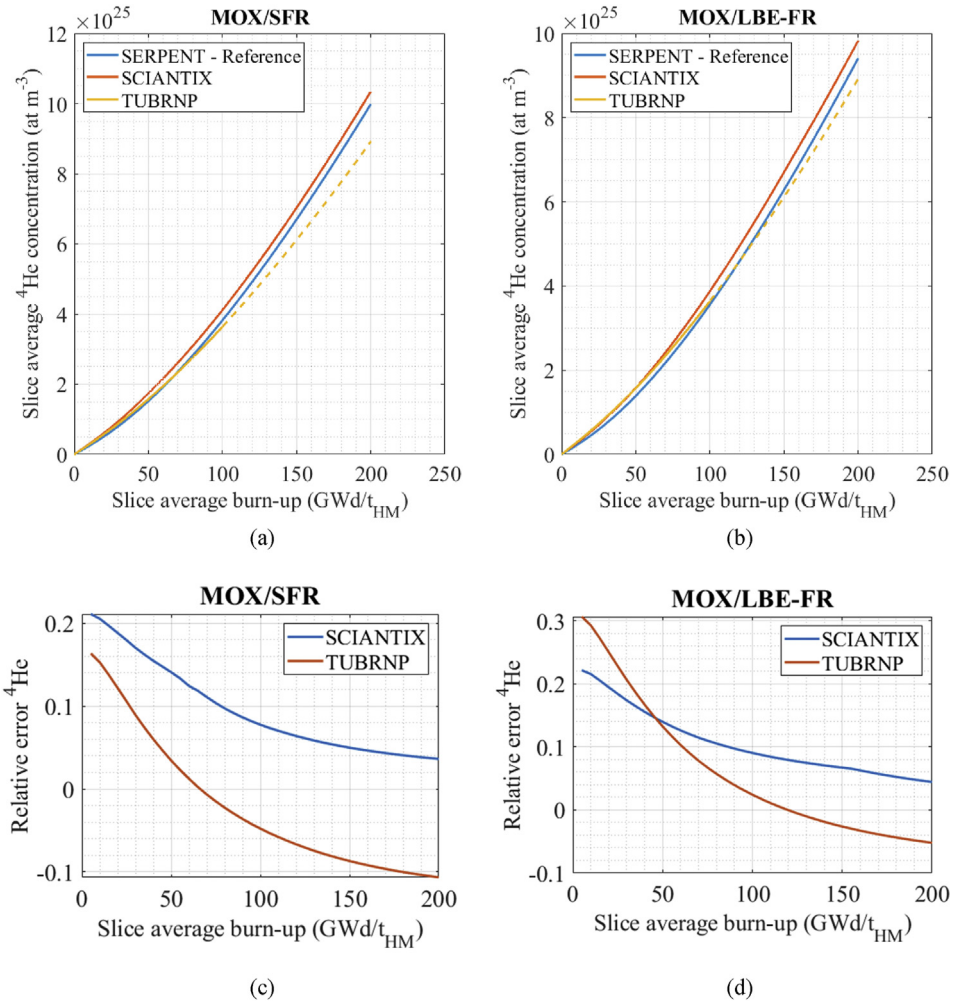

Fig. 3. Evolution of the concentration (at m^{-3}) of ^{4}He in (a) SFR case, (b) LBE-FR case. The result of TUBRNP is dashed above 100 GWd/t_{HM}, i.e., outside its verification range. The evolution of the normalized deviation of the SCIANTIX and TUBRNP results from the reference SERPENT results is reported as a function of burn-up for the (c) the SFR case and (d) the LBE-FR case.

Besides showing the agreement between the calculated helium and actinide concentrations, this benchmark has the purpose to compare the computational time of SCIANTIX and TUBRNP to prove the suitability of the developed module in the framework of fuel performance calculations. Table 3 shows that the SCIANTIX execution time is in line with TUBRNP for all the test cases, proving that SCIANTIX is sufficiently optimized to meet the time requirements of engineering-scale fuel performance codes.

SERPENT results are considered as high-fidelity reference to be compared to both SCIANTIX and TUBRNP results. To this purpose, the Root-Mean Square Error (*RMSE*) has been exploited as verification metric:

$$RMSE = \sqrt{\frac{1}{N}\sum_{n=1}^{N}\left(\frac{C_n - R_n}{R_n}\right)^2} \tag{9}$$

where C_i is the calculated value, R_i is the reference value, N is the number of burn-up steps and the summation is done for each burn-up step.

For each test-case, the calculated helium and actinide concentrations are presented in Figs. 3–8. For the sake of brevity, we report only the evolution with burn-up of the actinides directly contributing to helium production and of those nuclides initially present in the fuel.[9] From the observation of the nuclide profiles, SCIANTIX demonstrates a satisfactory agreement with the reference SERPENT model for every nuclide. Looking at the validation metric reported in Table 4, the general predictive capability of SCIANTIX is in line with that of TUBRNP for both test cases. It should be noticed that the TUBRNP module has been validated for FBR applications against experimental data up to 100 GWd/t_{HM} and it focuses only on the local concentrations of the most relevant nuclides, while SCIANTIX tracks the evolution in time of more nuclides, whose production affects the path to helium production.

Moreover, the new module shows a remarkable predictive capability for nuclides that present a non-zero concentration at the beginning of irradiation (i.e., ^{238}U and plutonium isotopes). Nuclides like ^{243}Pu, ^{241}Am and ^{244}Am present an appreciable *RMSE* because they are created by successive neutron capture reactions, whose cross-sections are affected by the error in the concentrations of the respective precursors.

The value of the branching ratio for the reaction

[9] The predicted concentration of ^{243}Pu is not shown because of its very low value in the fuel matrix at the end of irradiation ($<10^{21}$ at m^{-3}), but, in comparison with the SERPENT reference, it is still in line with the general behaviour of the new burn-up module.

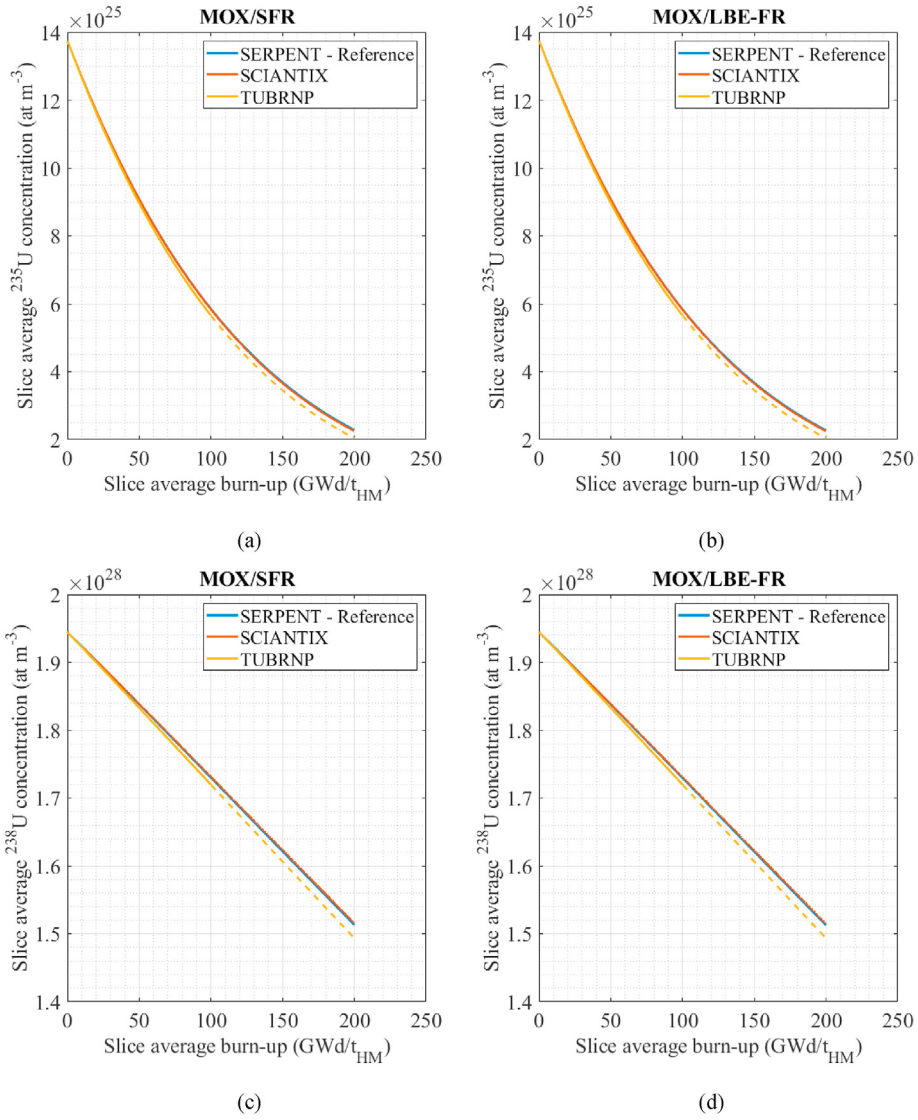

Fig. 4. Evolution of the concentration (at m^{-3}) of ^{235}U and ^{238}U in (a,c) SFR case, (b,d) LBE-FR case. The result of TUBRNP is dashed above 100 GWd/t$_{HM}$, i.e., outside its verification range.

^{241}Am(n,γ)^{242}Am has been derived from the SERPENT calculations (library JEFF-NDL-3.1) and set equal to 0.916 for both the MOX/SFR and MOX/LBE-FR cases [29]. These values are suitable for the ^{242}Am and ^{242m}Am predictions in both test cases, as shown by Table 4, indicating no deviation from the general trend of the module predictions for these two americium isotopes.

Lastly, since helium is produced by α-decays of several nuclides, it is expected that the error in the evaluation of the α-emitters propagates to the helium concentration. Fig. 3c and d show a satisfactory agreement between SCIANTIX and SERPENT with a normalized deviation comparable to TUBRNP one, proving that the set of burn-up and Pu/HM enrichment-dependent cross-sections is very effective in the description of the fuel evolution as burn-up increases. The presented methodology is therefore an improvement over the state-of-the-art, i.e., TUBRNP, which uses a single effective reactor-dependent cross-section value for each nuclear reaction. Nonetheless, the discrepancy between SCIANTIX and TUBRNP in the helium evolution prediction can be ascribed to several factors:

1) The reactor characteristics implemented in SERPENT impact on the neutron energy spectrum and on the normalization performed to obtain the one-group effective cross-sections. Thus, the value of the reaction cross-sections implemented in SCIANTIX can be in principle different from the ones implemented in TUBRNP. Nevertheless, the proposed methodology can be applied to derive look-up tables tailored to specific reactor designs.
2) According to Botazzoli [23], in TUBRNP the branching ratio of the reaction ^{241}Am(n,γ)^{242}Am is set equal to 0.85 for FBR applications. This value of the model parameter reduces the production of the α-emitters ^{242}Cm, ^{243}Cm and ^{238}Pu, and this reflects in a reduction of the helium concentration, whereas from Fig. 3c and d it is clear that SCIANTIX generally slightly overpredicts the helium concentration.
3) The value of the cross-section of the reaction ^{16}O(n,α)^{13}C is set ~ 1 mbarn in SCIANTIX as a direct result of the SERPENT energy-average. Since the value used in TUBRNP is 3.2 mbarn

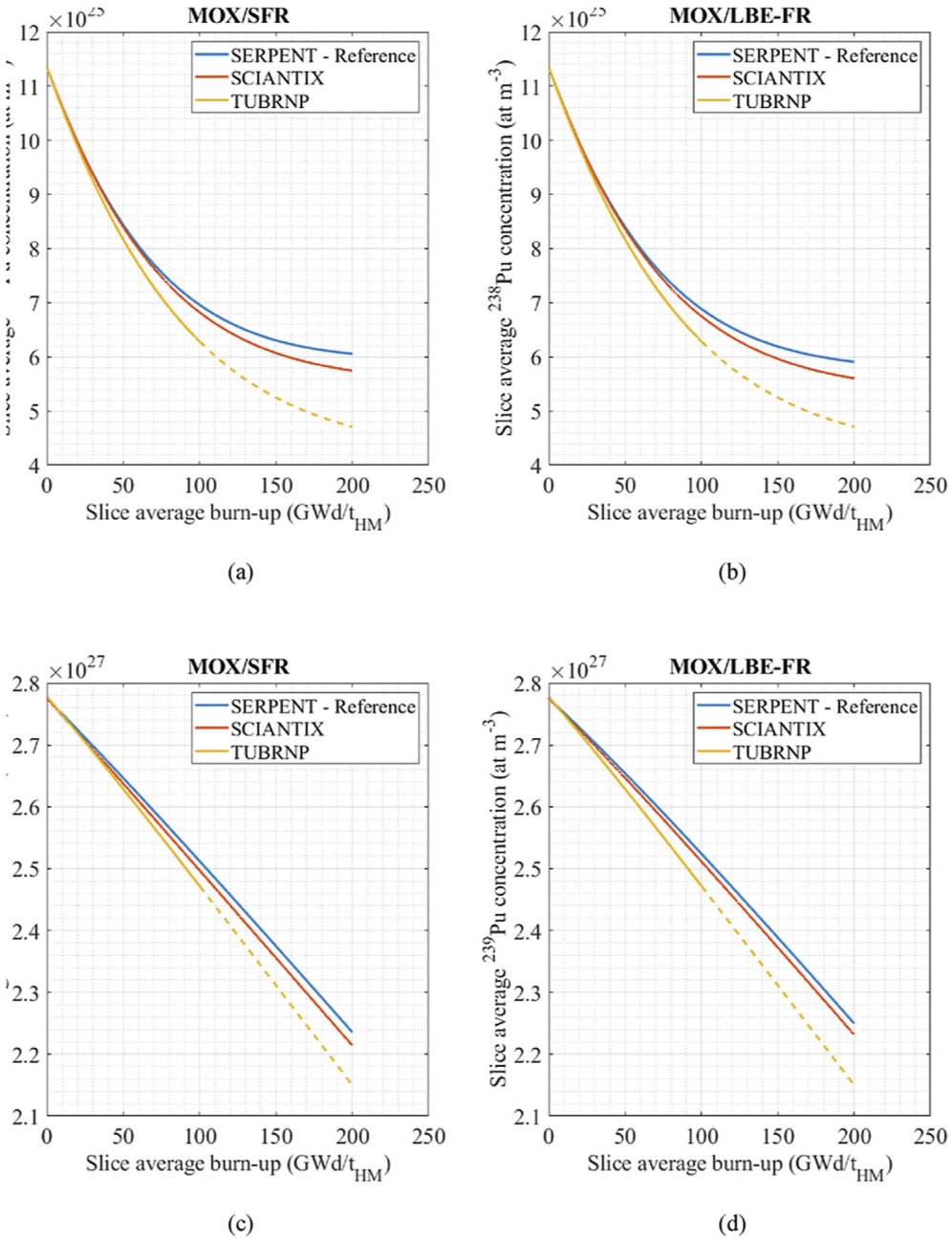

Fig. 5. Evolution of the concentration (at m^{-3}) of plutonium nuclides: ^{238}Pu, ^{239}Pu, ^{240}Pu, ^{241}Pu, ^{242}Pu in (a,c,e,g,i) SFR case, (b,d,f,h,l) LBE-FR case. The result of TUBRNP is dashed above 100 GWd/t_{HM}, i.e., outside its verification range.

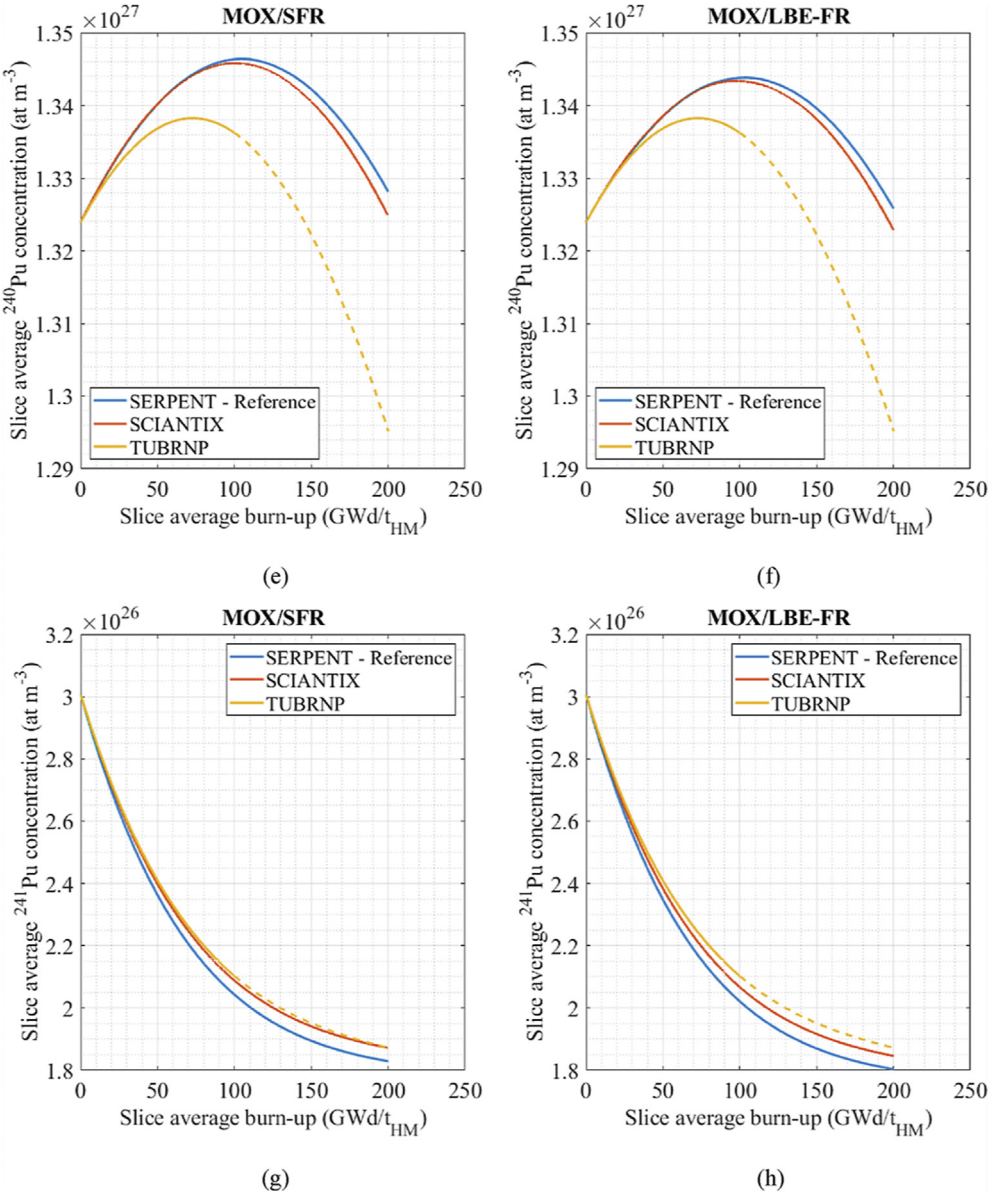

Fig. 5. (*continued*).

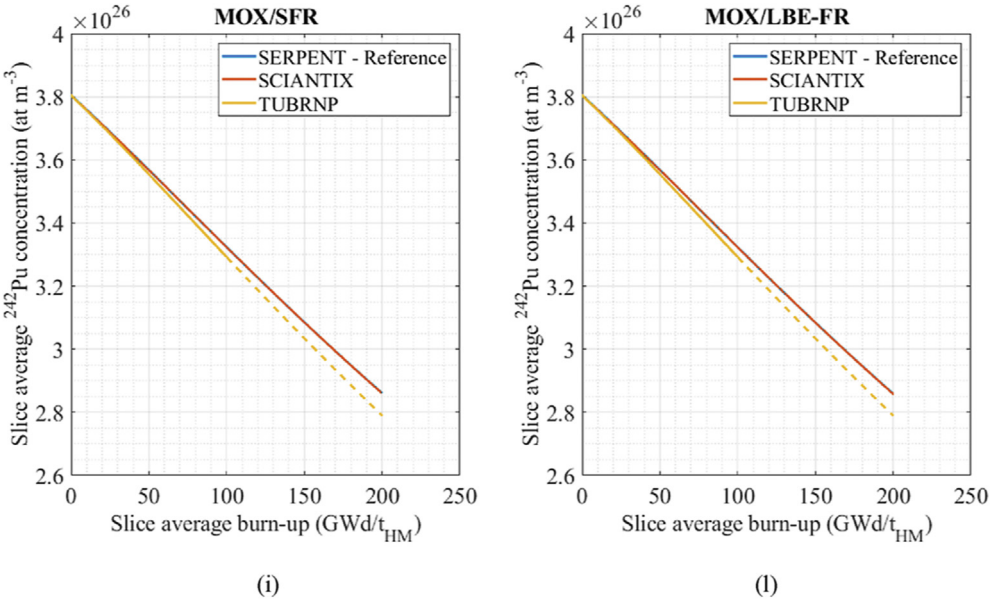

Fig. 5. (*continued*).

[23] we presume that this high value is used to compensate the general underprediction of curium nuclides by TUBRNP (Fig. 8).

Summarizing, the burn-up module presented in this work allows for an accurate evaluation of helium production in both SFR and LBE-FR conditions. This accuracy is achieved by a proper representation of the evolution of the actinides contributing to helium formation, tracking all the nuclides formed in the fuel up to ^{245}Cm. Moreover, the presented burn-up module has the advantage of being generalizable by applying the methodology described in Section 3 to any reactor/fuel combination and to specific reactor designs.

5. Conclusions

In this paper, we presented the development and assessment of a new burn-up module meant to be included in engineering-scale fuel performance codes. The module is able to calculate the helium evolution in mixed oxide fuels irradiated under fast neutron spectra, together with the concentration of 23 actinides.

We provided an in-depth view of the methodology applied for the evaluation of the reaction cross-sections, which is conceived to generate look-up tables for each cross-section as a function of burn-up and initial fuel Pu/HM enrichment. The cross-section values, corresponding to pairs of considered Pu/HM enrichment and burn-up, have been obtained from SERPENT, a high-fidelity Monte Carlo code. The generated look-up tables have been included in the SCIANTIX code, together with a dedicated solver for the depletion equations.

We herein assessed the burn-up module predictions for Pu-bearing oxide fuels in fast neutron spectra, considering two main cases representative of sodium and lead-bismuth eutectic fast

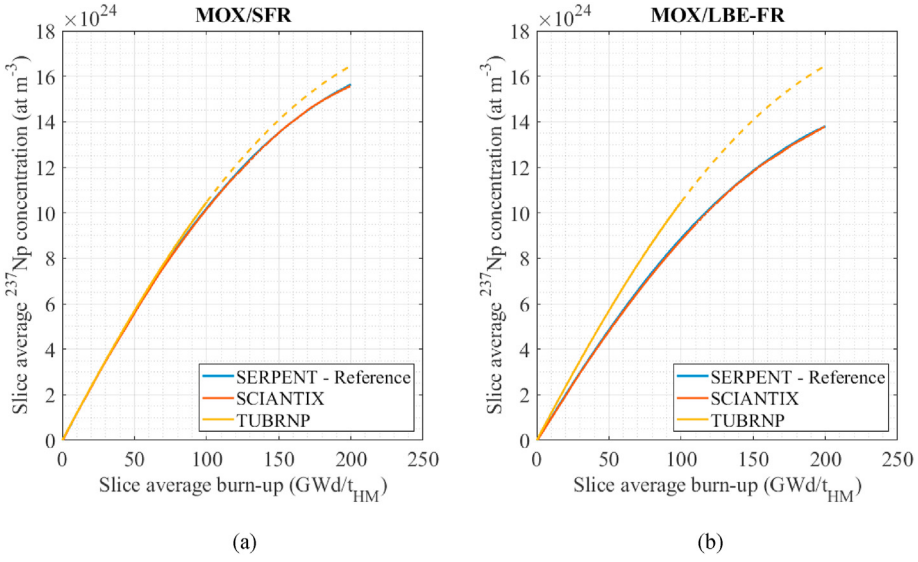

Fig. 6. Evolution of the concentration (at m^{-3}) of ^{237}Np in (a) SFR case, (b) LBE-FR case. The result of TUBRNP is dashed above 100 GWd/t$_{HM}$, i.e., outside its verification range.

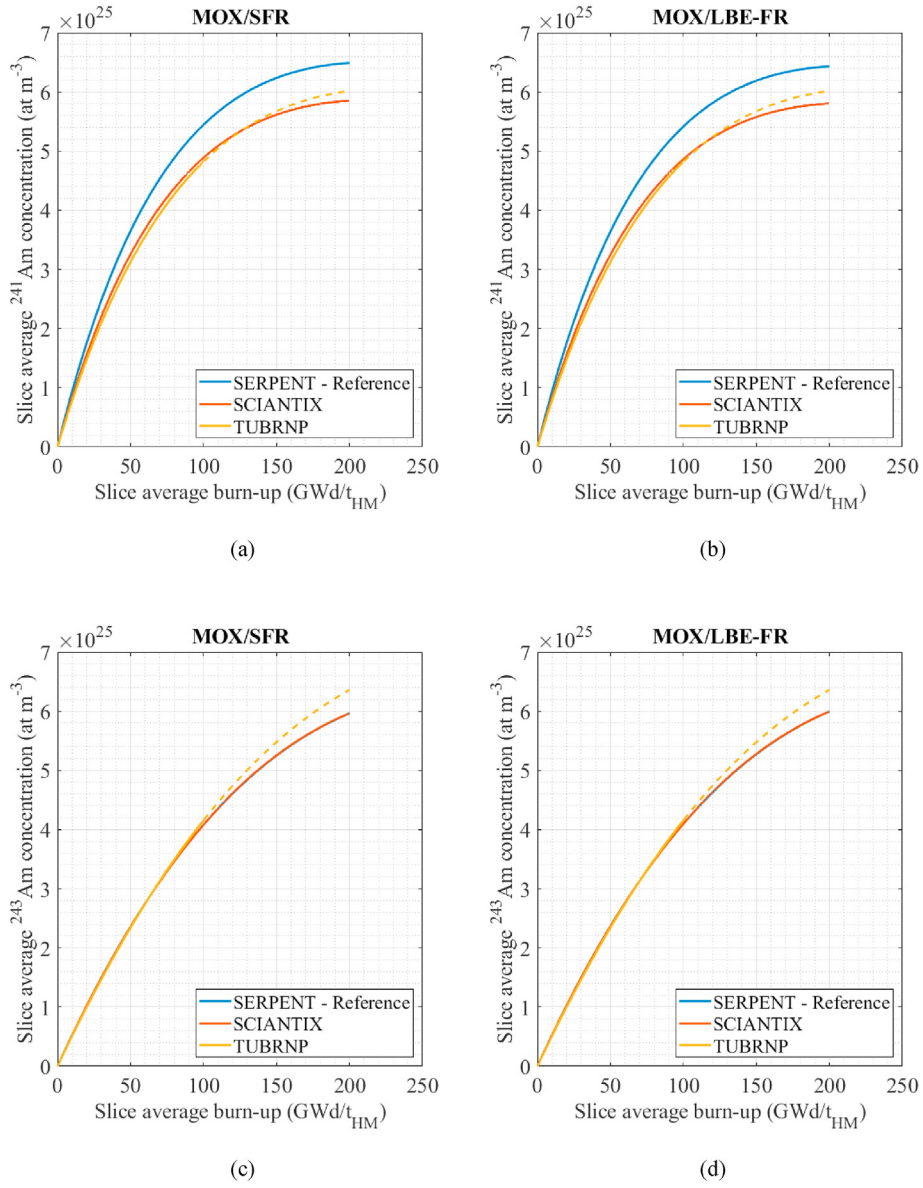

Fig. 7. Evolution of the concentration (at m^{-3}) of ^{241}Am and ^{243}Am in (a,c) SFR case, (b,d) LBE-FR case. The result of TUBRNP is dashed above 100 GWd/t_{HM}, i.e., outside its verification range.

reactor conditions. We compared the depletion calculations with the results obtained with SERPENT and TUBRNP, the burn-up model implemented in TRANSURANUS, using the root-mean square error as verification metric and relying on the SERPENT model as high-fidelity reference for both SCIANTIX and TUBRNP. Considering the results shown in this paper, the predictive capability of the new burn-up module is in line with state-of-the-art approaches, indicating that the herein presented burn-up module allows a reliable and accurate prediction of helium production in oxide fuels through the consistent tracking of a set of relevant actinides. Further comparison with experimental data [30] or code-to-code comparison (e.g., with ORIGEN) are foreseen and will be useful to strengthen the results of the presented module.

The burn-up module is designed to minimize the computational time, thus being applicable in engineering-scale fuel performance codes. A low computational time is achieved by selecting only relevant nuclear reactions and limiting the number of nuclides considered to those required for the accurate prediction of helium production. The solution of the depletion equations is achieved via an implicit numerical scheme allowing for robust and stable solution. Moreover, since the methodology relies on cross-section libraries derived from another code, generating new cross-sections for different types of reactor is a repeatable operation, making this methodology flexible for the analysis of any fuel/reactor combination, beyond the scope of the present work.

Future developments of the presented burn-up module will lead to the inclusion of fission products relevant for fuel performance calculations, such as noble gases, volatile fission products, elements

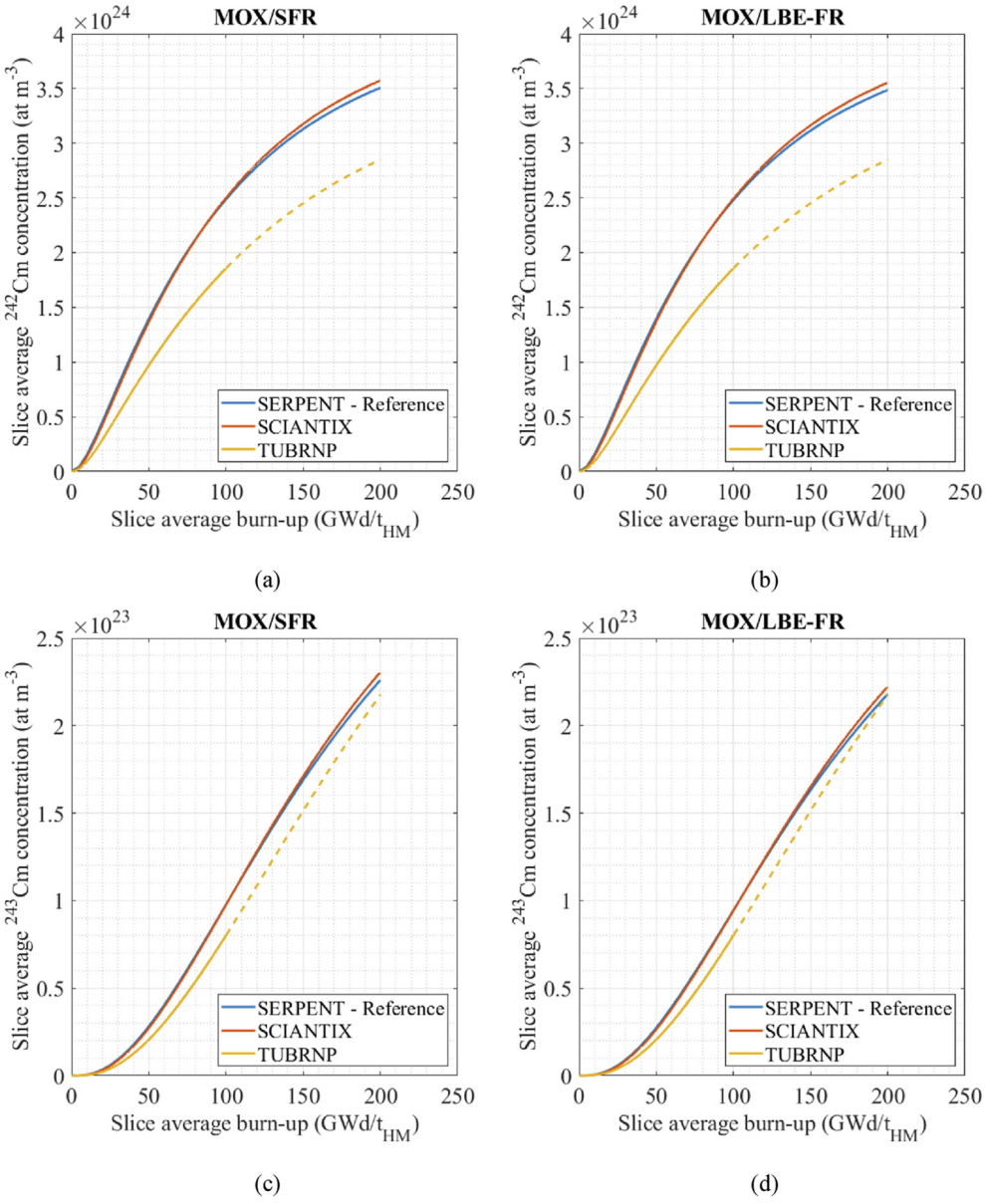

Fig. 8. Evolution of the concentration (at m^{-3}) of ^{242}Cm, ^{243}Cm, ^{244}Cm, ^{245}Cm in (a,c,e,g) SFR case, (b,d,f,h) LBE-FR case. The result of TUBRNP is dashed above 100 GWd/t_{HM}, i.e., outside its verification range.

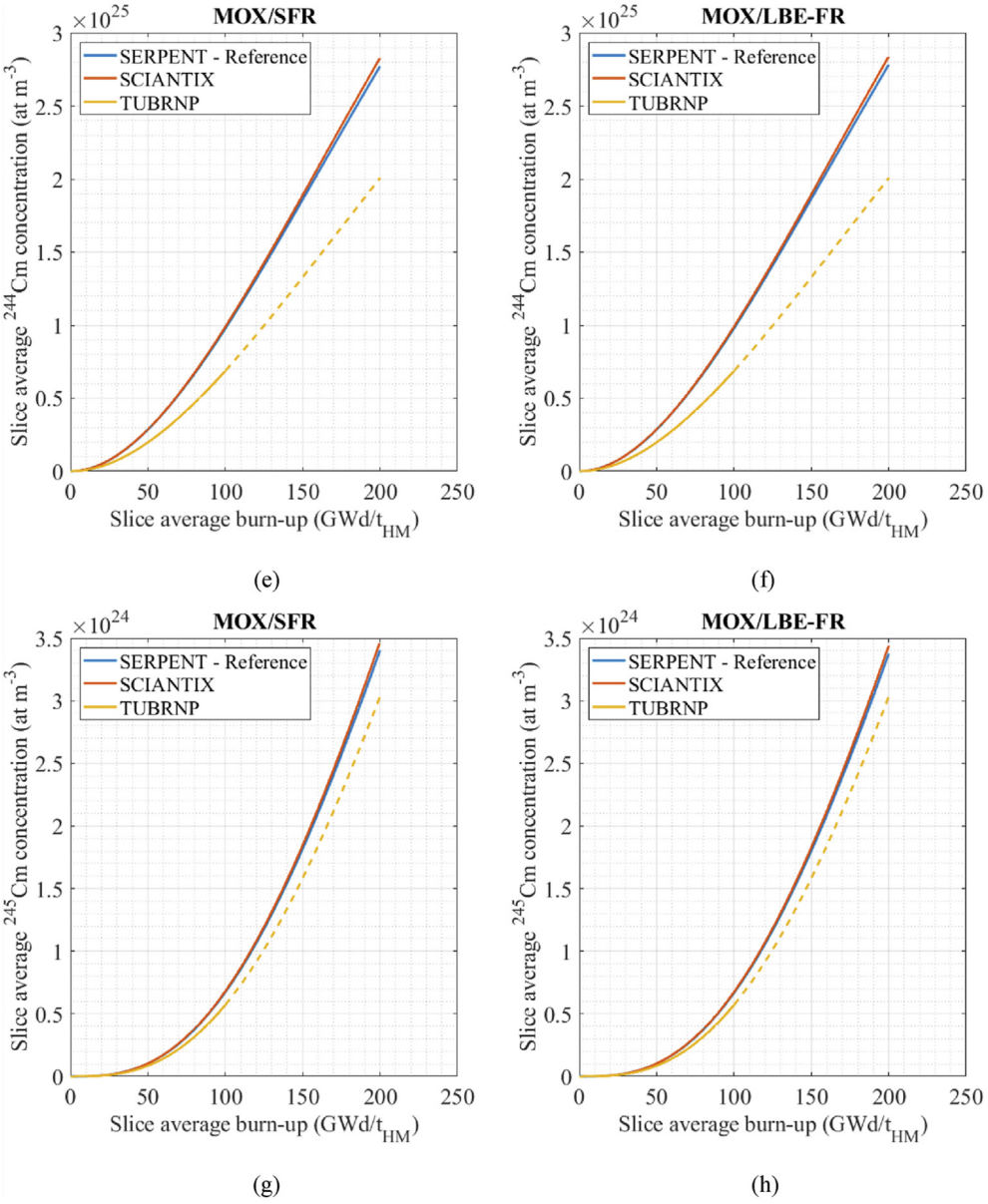

Fig. 8. (*continued*).

Table 4
Verification metric (Root-Mean Square Error) for the comparison of the new burn-up model and the SERPENT reference. The nuclides contributing directly to helium production via α-decay are marked in bold. The verification metric is reported also for the results from the TRANSURANUS burn-up module (TUBRNP), for the sake of comparison. It should be noted that the evaluation of the verification metric for TUBRNP includes the range 100–200 GWd/t_{HM}, in which the model is not validated. Lower values of the verification metric correspond to a better agreement.

RMSE (/)	MOX/SFR		MOX/LBE-FR	
	SCIANTIX	TUBRNP	SCIANTIX	TUBRNP
^{4}He	0.1080	0.0817	0.1148	0.1194
^{234}U	**0.1194**	**-**	**0.1194**	**-**
^{235}U	**0.0055**	**0.0510**	**0.0049**	**0.0487**
^{236}U	**0.0059**	**0.0813**	**0.0061**	**0.0708**
^{237}U	0.1392	–	0.1408	–
^{238}U	**0.0010**	**0.0072**	**0.0009**	**0.0070**
^{237}Np	**0.0045**	**0.0328**	**0.0097**	**0.1841**
^{238}Np	0.1296	–	0.1232	–
^{239}Np	0.1193	–	0.1210	–
^{238}Pu	**0.0276**	**0.1251**	**0.0274**	**0.1135**
^{239}Pu	**0.0063**	**0.0206**	**0.0053**	**0.0250**
^{240}Pu	**0.0011**	**0.0119**	**0.0009**	**0.0105**
^{241}Pu	0.0200	0.0247	0.0204	0.0353
^{242}Pu	**0.0002**	**0.0128**	**0.0002**	**0.0126**
^{243}Pu	0.1318	–	0.1316	–
^{241}Am	**0.1029**	**0.1186**	**0.1024**	**0.1148**
^{242}Am	0.0179	–	0.0178	–
^{242m}Am	0.1007	–	0.1017	–
^{243}Am	**0.0004**	**0.0340**	**0.0007**	**0.0311**
^{244}Am	0.2148	–	0.2165	–
^{242}Cm	**0.0296**	**0.2665**	**0.0293**	**0.2654**
^{243}Cm	**0.0336**	**0.2112**	**0.0325**	**0.1910**
^{244}Cm	**0.0135**	**0.2930**	**0.0132**	**0.2946**
^{245}Cm	**0.0133**	**0.1534**	**0.0129**	**0.1471**

forming metallic or oxide inclusions in nuclear fuels, and those soluble in the fuel matrix. Moreover, the application of the present methodology to other fuel/reactor concepts, namely, to uranium oxide fuel and MOX fuel in light water reactor conditions is currently ongoing and will constitute the natural step for a more comprehensive showcase of the methodology.

Declaration of competing interest

The authors declare that they have no known competing financial interests or personal relationships that could have appeared to influence the work reported in this paper.

Acknowledgments

This research has received funding from the Euratom research and training programme 2014–2018 through the INSPYRE Project under grant agreement No. 754329.

References

[1] D.R. Olander, Fundamental Aspects of Nuclear Reactor Fuel Elements, Technical Information Center – Energy Research and Development Administration, University of California, Berkeley, 1976.
[2] J. Rest, M.W.D. Cooper, J. Spino, J.A. Turnbull, P. Van Uffelen, C.T. Walker, Fission gas release from UO_2 nuclear fuel: a review, J. Nucl. Mater. 513 (2019) 310–345.
[3] P. Van Uffelen, R.J.M. Konings, C. Vitanza, J. Tulenko, Analysis of reactor fuel rod behavior, Handb. Nucl. Eng. (2010) 1519–1627.
[4] P. Van Uffelen, J. Hales, W. Li, G. Rossiter, R. Williamson, A review of fuel performance modelling, J. Nucl. Mater. 516 (2019) 373–412.
[5] J.E. Kelly, Generation IV International Forum: a decade of progress through international cooperation, Prog. Nucl. Energy 77 (2014) 240–246.
[6] GIF (Generation IV International Forum), Annual Report 2019, OECD/NEA No. 7527, 2019.
[7] J.F. Briesmeister, MCNP4C - A General Monte Carlo N Particle Transport Code, Manual LA–13709–M, 2000.
[8] L.C. Leal, O.W. Hermann, S.M. Bowman, C.V. Parks, Automatic rapid process for the generation of problem-dependent SAS2H/ORIGEN-S cross-section libraries, Nucl. Technol. 127 (1) (1999) 1–23.
[9] I. Palmer, K.W. Hesketh, P.A. Jackson, A model for predicting the radial power profile in a fuel pin. in: IAEA specialists meeting on water reactor fuel element performance computer modelling, Preston, United Kingdom, 15-19 March 1982, IAEA, 1983.
[10] K. Lassmann, TRANSURANUS: a fuel rod analysis code ready for use, Nucl. Mater. Fission React. (1992) 295–302.
[11] K. Lassmann, C. O'Carroll, J. van de Laar, C.T. Walker, The radial distribution of plutonium in high burnup UO_2 fuels, J. Nucl. Mater. 208 (3) (1994) 223–231.
[12] A. Schubert, P. Van Uffelen, J. van de Laar, C.T. Walker, W. Haeck, Extension of the TRANSURANUS burn-up model, J. Nucl. Mater. 376 (1) (2008) 1–10.
[13] European Commission, TRANSURANUS Handbook, in: Joint Research Centre Directorate G - Nuclear Safety & Security, "Transuranus Handbook, 2018. Karlsruhe, Germany.
[14] J.I. Tijero Cavia, A. Schubert, P. Van Uffelen, P. Poeml, S. Brémier, J. Somers, M. Seidl, R. Macian-Juan, The TRANSURANUS burn-up model for thorium fuels under LWR conditions, Nucl. Eng. Des. 326 (2018) 311–319. November 2017.
[15] C.B. Lee, D.H. Kim, J.S. Song, J.G. Bang, Y.H. Jung, RAPID model to predict radial burnup distribution in LWR UO_2 fuel, J. Nucl. Mater. 282 (2–3) (2000) 196–204.
[16] S. Lemehov, J. Nakamura, M. Suzuki, PLUTON: a three-group model for the radial distribution of plutonium, burnup, and power profiles in highly irradiated LWR fuel rods, Nucl. Technol. 133 (2) (2001) 153–168.
[17] S.Y. Kurchatov, V.V. Likhanskii, A.A. Sorokin, O.V. Khoruzhii, RTOP-code simulation of the radial distribution of heat release and plutonium isotope accumulation in high burnup oxide fuel, At. Energy 92 (4) (2002) 349–356.
[18] B.H. Lee, Y.H. Koo, J.Y. Oh, J.S. Cheon, D.S. Sohn, Improvement of fuel performance code COSMOS with recent in-pile data for MOX and UO_2 fuels, Nucl. Technol. 157 (1) (2007) 53–64.
[19] A. Soba, A. Denis, Simulation with DIONISIO 1.0 of thermal and mechanical pellet-cladding interaction in nuclear fuel rods, J. Nucl. Mater. 374 (1–2) (2008) 32–43.
[20] A. Soba, A. Denis, L. Romero, E. Villarino, F. Sardella, A high burnup model developed for the DIONISIO code, J. Nucl. Mater. 433 (1–3) (2013) 160–166.
[21] A. Soba, A. Denis, DIONISIO 2.0: new version of the code for simulating a whole nuclear fuel rod under extended irradiation, Nucl. Eng. Des. 292 (2015) 213–221.
[22] E. Federici, A. Courcelle, P. Blanpain, H. Cognon, Helium production and behavior in nuclear oxide fuels during irradiation in LWR, in: in: Proceedings of the 2007 International LWR Fuel Performance Meeting, San Francisco, California, USA, 30 September - 3 October 2007, American Nuclear Society, 2007, pp. 664–673.
[23] P. Botazzoli, L. Luzzi, S. Brémier, A. Schubert, P. Van Uffelen, C.T. Walker, W. Haeck, W. Goll, Extension and validation of the TRANSURANUS burn-up model for helium production in high burn-up LWR fuels, J. Nucl. Mater. 419 (1–3) (2011) 329–338.
[24] D. Pizzocri, T. Barani, L. Luzzi, SCIANTIX: a new open source multi-scale code for fission gas behaviour modelling designed for nuclear fuel performance codes, J. Nucl. Mater. (2020) 152042.
[25] EERA-JPNM, INSPYRE: Investigations Supporting MOX fuel licensing in ESNII prototype Reactors [Online]. Available: http://www.eera-jpnm.eu/inspyre/, 2017.
[26] J. Leppänen, M. Pusa, T. Viitanen, V. Valtavirta, T. Kaltiaisenaho, The SERPENT Monte Carlo code: status, development and applications, in: in: SNA + MC 2013 - Joint International Conference on Supercomputing in Nuclear Applications + Monte Carlo, Paris, France, 27-31 October 2013, OECD/NEA, 2014.
[27] D. Pizzocri, T. Barani, L. Luzzi, Coupling of TRANSURANUS with the SCIANTIX fission gas behaviour module, Int. Work. "Towards Nucl. fuel Model. Var. React. types across Eur. (2019).
[28] P. Van Uffelen, A. Schubert, L. Luzzi, T. Barani, A. Magni, D. Pizzocri, M. Lainet, V. Marelle, B. Michel, B. Boer, S. Lemehov, A. Del Nevo, D7.2 - Incorporation and verification of models and properties in fuel performance codes, INSPYRE Deliverable D7.2 (2020). http://www.eera-jpnm.eu/inspyre/filesharer/documents/Deliverables%20&%20Milestones/Public%20deliverables.
[29] P. Talou, T. Kawano, P.G. Young, M.B. Chadwick, R.E. MacFarlane, Improved evaluations of neutron-induced reactions on americium isotopes, Nucl. Sci. Eng. 155 (1) (2007) 84–95.
[30] P. Botazzoli, Helium Production and Behaviour in LWR Oxide Nuclear Fuels, PhD Thesis, Politecnico di Milano, Italy, 2011.
[31] K. Tasaka, J. Katakura, H. Ihara, T. Yoshida, S. Iijima, R. Nakasima, T. Nakagawa, H. Takano, JNDC Nuclear Data Library of Fission Products - Second Version, JAERI 1320, 1990.

[32] S. Pearlstein, Analysis of (n,2n) cross sections for medium and heavy mass nuclei, Nucl. Sci. Eng. 23 (3) (1965) 238–250.
[33] J. Frehaut, A. Bertin, R. Bois, Measurement of the ^{235}U(n,2n) cross section between threshold and 13 MeV, Nucl. Sci. Eng. 74 (1) (1980) 29–33.
[34] H. Aït Abderrahim, P. Baeten, D. De Bruyn, R. Fernandez, MYRRHA - a multi-purpose fast spectrum research reactor, Energy Convers. Manag. 63 (2012) 4–10.
[35] M. Pusa, Numerical Methods for Nuclear Fuel Burnup Calculations, 2013.
[36] V. Sobolev, Database of thermophysical properties of liquid metal coolants for GEN-IV, SCK• CEN Tech. Report SCKCEN-BLG-1069 16 (12) (2010) 3496–3502.
[37] S.M. Bowman, M.D. DeHart, C.V. Parks, Validation of SCALE-4 for burnup credit applications, Nucl. Technol. 110 (1) (1995) 53–70.
[38] A. Alfonsi, C. Rabiti, A.S. Epiney, Y. Wang, J. Cogliati, Phisics toolkit: multi-reactor transmutation analysis utility - MRTAU, in: Int. Conf. PHYSOR 2012: Advances in Reactor Physics, American Nuclear Society, 2012, pp. 2181–2195.
[39] S. Höglund, J. Kristensson, ESSANUF - European Supply of SAfe NUclear Fuel. International conference on WWER fuel performance, modelling and experimental support, Nesebar, Bulgaria, 16-23 September 2017, IAEA, 2017.
[40] C. Demazière, V.H. Sanchez-Espinoza, B. Chanaron, Advanced Numerical Simulation and Modelling for Reactor Safety – Contributions from the CORTEX, HPMC, McSAFE and NURESAFE projects. 9th European Commission Conferences on EURATOM Research and Training in Safety of Reactor Systems and Radioactive Waste Management (FISA 2019 - Euradwaste' 19), Pitesti, Romania, 4-7 June 2019, Euratom, 2019.
[41] M. Herman, A. Trkov, "ENDF-6 formats manual: data formats and procedures for the evaluated nuclear data file ENDF", B-VI ENDF/BVII (Report BNL-90365-2009 Rev.1), Natl. Nucl. Data Center (2009). https://www.oecd-nea.org/dbdata/data/manual-endf/endf102.pdf.